IBRACON Structures and Materials Journal
Revista IBRACON de Estruturas e Materiais
ISSN 1983-4195 ismj.org

ORIGINAL ARTICLE

# Computational modeling of structural masonry shear walls considering cracking effects at mortar joints

## *Modelagem computacional de paredes de contraventamento de alvenaria estrutural considerando os efeitos de fissuração nas juntas de argamassa*

Nicole Nahara Souza de Oliveira[a]
Joel Araújo do Nascimento Neto[a]
Guilherme Aris Parsekian[b]

[a]Universidade Federal do Rio Grande do Norte – UFRN, Programa de Pós-graduação em Engenharia Civil, Natal, RN, Brasil
[b]Universidade Federal de São Carlos – UFSCar, Programa de Pós-graduação em Engenharia Civil, São Carlos, SP, Brasil

Received 24 October 2021
Accepted 22 November 2022

**Abstract:** This study presents a computational model to analyze structural masonry shear walls behavior considering the effects of mortar joint cracking on loss of stiffness. The simplified equivalent frame model was used but including link elements between the frame node to simulate the effects of cracking. The analyses were conducted using the SAP2000 computer program and consisted of modeling four shear walls on a 1/3 scale which were experimentally assessed. The results indicated that the proposed computational modeling approach consistently reproduced the effects of cracking at mortar joints, accurately simulating the nonlinear behavior of masonry.

**Keywords:** structural masonry, shear wall, computational modeling, equivalent frame method (EqFM), nonlinear analysis, cracking effects.

**Resumo:** O presente trabalho consistiu na elaboração de um modelo computacional para avaliar o comportamento de paredes de contraventamento de alvenaria estrutural de blocos considerando-se os efeitos da fissuração das juntas de argamassa na perda de rigidez. Com esse intuito foi utilizado o modelo simplificado de barras equivalentes, incluindo-se elementos de ligação entre as barras para simular numericamente os efeitos da fissuração. As análises foram realizadas utilizando-se o programa computacional SAP2000 e consistiram na modelagem de quatro paredes de contraventamento na escala 1/3 que foram ensaiadas experimentalmente. Os resultados indicaram que a modelagem computacional idealizada reproduziu de forma consistente os efeitos da fissuração na junta de argamassa, simulando adequadamente o comportamento não linear da alvenaria.

**Palavras-chave:** alvenaria estrutural, paredes de contraventamento, modelagem computacional, modelo de barras equivalentes (MBEq), análise não-linear, efeitos de fissuração.

**How to cite:** N. N. S. Oliveira, J. A. Nascimento Neto, and G. A. Parsekian, "Analysis of structural masonry shear walls considering the cracking effects," *Rev. IBRACON Estrut. Mater.*, vol. 16, no. 4, e16410, 2023, https://doi.org/10.1590/S1983-41952023000400010

## 1. INTRODUCTION

The structural masonry construction system has been widely used throughout Brazil over the past few years, due to its proven benefits such as speed in construction, economy of materials and improvement of workmanship. Experimental, theoretical and/or numerical studies on structural masonry buildings have been developed concurrently with its increasing use, contributing to a better understanding of how these structures behave and thereby optimizing construction processes and design.

**Corresponding author:** Nicole Nahara Souza de Oliveira. E-mail: nicolenahara@hotmail.com
**Financial support:** The author gratefully acknowledges the support of the Civil Engineering Graduate Program of the Federal University of Rio Grande do Norte. This paper was financed in part by the Coordenação de Aperfeiçoamento de Pessoal de Nível Superior (CAPES) - Financing Code 001.
**Conflict of interest:** Nothing to declare.
**Data Availability:** the data that support the findings of this study are available from the corresponding author, NNSO, upon reasonable request.

Computational modeling is a valuable tool, since it allows the evaluation of different wall configurations subjected to different support conditions, applied load and analysis criteria. Computational models are usually validated by experimental tests, which, in turn, represent the characteristics of the structure under study. The present study aimed to evaluate the accuracy of the equivalent frame method (EqFM) computational model, developed by Nascimento et al. [1], to simulate the cracking effects of structural masonry walls in the building bracing system. The classic frame model was modified to allow simulation of the cracking nonlinear effects. The results of experimental tests reported by Nascimento [2] were used to validate the model. This study is justified by the fact that the loss of stiffness associated with shear wall cracking is still not fully understood by the technical-scientific community, and to allow better structural design of masonry buildings.

## 2 THEORETICAL FRAMEWORK

### 2.1 Shear walls in structural masonry buildings

In structural masonry buildings, shear walls are responsible for the overall stability of the building, providing rigidity and resistance to horizontal and vertical forces.

Parsekian et al. [3] reported that shear walls with a predominant length in the two main directions are necessary to provide rigidity to the building. According to Paes [4], these walls can be classified into those that brace the structure and those that are braced by other structural members. Despite being part of the structure, the element that is braced plays a minimal role in resistance when subjected to horizontal forces. On the other hand, bracing walls provide stability to the structure and resist the internal forces arising from the action of horizontal forces.

According to Parsekian et al. [3] and Mata [5], the behavior of these walls depends on several factors, such as boundary conditions and type of connections, magnitude of applied loads, type of materials used, type of masonry (reinforced or unreinforced), wall dimension, and existence of openings (doors and/or windows), among others. Nascimento [6] remarks that the resistance of a bracing wall is dependent on the stiffness developed in its own plane, meaning that stiffness to displacements outside this plane are neglectable. This aspect is of considerable importance in the behavior of the bracing walls when incorporating transverse walls as flanges.

### 2.2 Nonlinearity in structural masonry

Gomes [7] reports that a satisfactory nonlinear analysis of masonry must include the nonlinear behavior of the material, such as cracking, softening and hardening behavior, multiaxial stress states, and the behavior of the contact interface between block and mortar, including cracking. For these reasons, non-linear analyses of structural masonry are essential to validate theoretical models, to a better understanding how the structure behaves and conduct novel studies in this area.

According to Peleteiro [8], the nonlinear behavior of masonry is caused primarily by two effects: progressive rupture and nonlinear characteristics of the constituent materials. For the material model to represent the behavior of the masonry, both effects must be included. According to Andreaus [9], the failure of masonry walls subjected to loads in their own plane may be attributed to three basic mechanisms: sliding of the horizontal mortar joints, cracking of the units/blocks and splitting of the vertical mortar joint.

Most nonlinear models use so-called micro-modeling, which is characterized by the separate discretization of the units/blocks and the mortar, and, in some cases, the interface between them. However, this type of modeling only applies to analysis of small elements to assess the localized behavior of the masonry, as in the study of prisms and small walls. When a larger region of the structure is modeled to assess the global behavior, the best option is to use macro-modeling, where the masonry is treated as homogenized material whose mechanical and elastic properties are equivalent to the average characteristics of a given non-homogeneous material.

Examples of this type of modeling can be found in the studies of van Zijl [10], Garbor et al. [11] and Zucchini and Lourenço [12]. These studies are based on numerical models with results compared to experimental models of masonry panels subjected to horizontal forces. In all the studies, the authors performed micro-modeling of the masonry, with separate discretization of the block and mortar elements, attributing to them the specific properties of each material to simulate the masonry nonlinear behavior of individual panels. In the case of several wall members, such as those in building analysis, the use of micro-modeling is not adequate due to the number of unknowns in the numerical solution. In this case, the use of macro-modeling is preferable, as can be seen in the studies of Medeiros [13] and Lopes [14], who conducted linear analysis.

The study of Belmouden and Lestuzzi [15] is another example of macro-modeling application. The authors presented an equivalent planar-frame model with openings validated by an experimental study. The model deals with seismic analysis using the Pushover method for masonry and reinforced concrete buildings. In the model, based on the finite element method, were inserted nonlinear flexural springs at the ends of the piers and spandrel elements. For the development of capacity curves, the obtained results from the proposed model showed good agreement with experimental results.

The study of Voon and Ingham [16] presents two types of strut-and-tie models to evaluate wall strength compared with experimental tests. The first type was a simplified strut-and-tie model, which assumed that all panels were pinned at the bond beam center and that lateral force was applied to the bracing panels at the center of the bond beam. A second set of strut-and-tie models considered the lateral force to be applied as a single point load at the center of the wall top. Strength prediction by the simplified strut-and-tie method was found to closely match the test results of masonry walls with a single opening, but significant underestimation of strength by this method was found for walls with two openings.

In a recent study, Pirsaheb et al. [17] developed a model established on truss elements which have been improved in a second study reported by Pirsaheb et al. [18]. In both the models, namely Multi-Pier-Macro (MPM), the masonry is simulated by an assemblage of pier (vertical trusses) and diagonal connecting elements (braces). A validation analysis to correctly reproduce masonry behavior under axial loads, combined shear and compression stresses and bending and shear actions were developed. In sequence, four masonry full scale shear walls with different length to width ratios and presence or absence of openings were analyzed in the non-linear static range. The results obtained showed good agreement to experimental tests simulating in each step of loading the spreading and position of tensile and shear cracks.

### 2.3 Equivalent frame method (EqFM)

An experimental study of shear walls requires a high-quality laboratory, which is why so much experimental research use small scale models, given their large actual dimensions and the need for robust equipment. After proper calibration, computational modeling may become an alternative to experimental studies since computational resources are essential to research development. Thus, the present study consisted of evaluating a computational model that simulated the lack of stiffness resulting from the cracking of walls subjected to horizontal forces.

The equivalent frame method (EqFM), developed by Nascimento et al. [1], uses beam elements to discretize the wall and simulate stiffness in its own plane, thereby distributing stresses and strains in the masonry. This model was initially calibrated by Medeiros [13], Lopes [14] and Barbosa [19], albeit conducting linear analyses.

According to Medeiros [13], the discretization adopted in the model consists of arranging vertical bars in the hollows of the blocks and horizontal bars at the level of each course, considering the gross or net area of the masonry for both bars. In sections that exhibit grouting, the corresponding effect of increasing stiffness may be considered when adopting the modulus of elasticity of grouted masonry, even if the reference area is the gross section. Figure 1 illustrates a masonry wall discretized using the equivalent frame method (EqFM), showing the distribution of the bars and their position coincident with the center of gravity of the hollow blocks. In this numerical model the bars are represented by classical beam elements with six degrees of freedom in the ends and linear approximation for the displacements function. The specific properties of each bar are presented in the following.

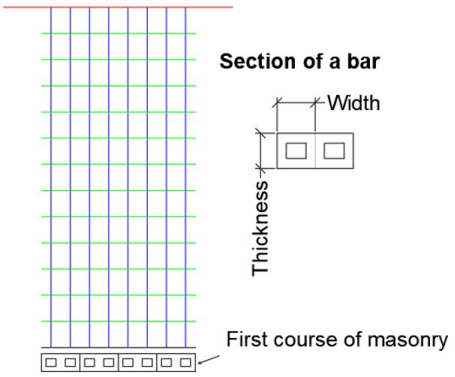


**Figure 1.** Discretization of a masonry wall using the equivalent frame method (EqFM).

### 2.4 Link elements in modeling

Link elements can be used in computational modeling to simulate the interaction at the interface between distinct parts of a structural member and may also be interpreted as contact nonlinearity. The link element used by Guerrante [20] to simulate cracking in reinforced concrete beams was the equivalent of six independent springs, one for each of the six degrees of freedom of deformation (one translation and one rotation along the normal axis of the contact plane, two translations and two rotations along the axes contained in the contact plane). The author studied the reinforcement of these beams using three-dimensional finite elements in the discretization, and GAP-type link elements, implemented in the SAP2000 software model library, which were arranged between the solid elements used in the beam simulation and the elements of reinforcement. The analysis consisted of comparing the numerical models developed by Guerrante [20] and the experimental results from Simões [21]. The results indicated that the modeling carried out by the author [20] was satisfactory, and all the elements used in the model adequately simulated the behavior observed in the experiment.

## 3 METHODOLOGY

The SAP2000 program was used to build the computational modeling of four walls selected from Nascimento [2]. The equivalent frame method (EqFM) was used, with the addition of link elements to simulate cracking in mortar joints.

### 3.1 Description of tests performed by Nascimento [2]

Nascimento [2] conducted tests with different configurations of 1:3 small scale walls. Of the walls evaluated, those denominated PISG1, PICG1, PPSG1 and PPCG1 were selected for computational modeling. Walls that did not display an opening were denominated individual walls, also used in the following analyses, whose dimensions in centimeters are shown in Figure 2. The PISG1 wall represents an unreinforced masonry wall, and PICG1 a reinforced masonry wall with grouting at the ends. Figure 2c illustrates part of the instrumentation used in the tests for measuring horizontal displacements. The horizontal displacements measured by transducers T1 and T2 were used for comparison purposes with computational models. In the walls, reinforced concrete elements (slab strips) were placed at the base and at the top to improve the distribution of vertical and horizontal forces.

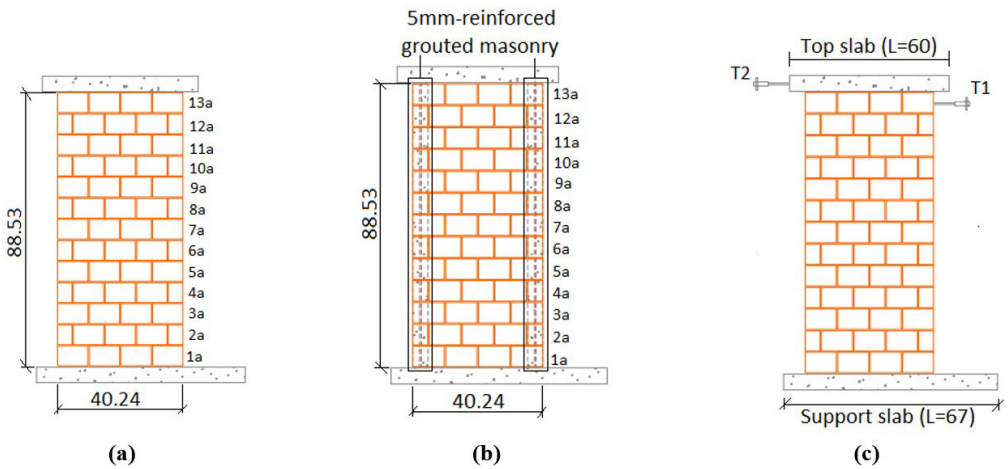


**Figure 2.** Individual shear wall (dimensions in centimeters). (a) PISG1 Wall; (b) PICG1 Wall; (c) Displacement measurement locations. (Source: adapted from Nascimento [2]).

Figure 3 illustrates the geometry, grouting locations, and part of the instrumentation used in the tests to measure the horizontal displacements of walls with typical door opening.

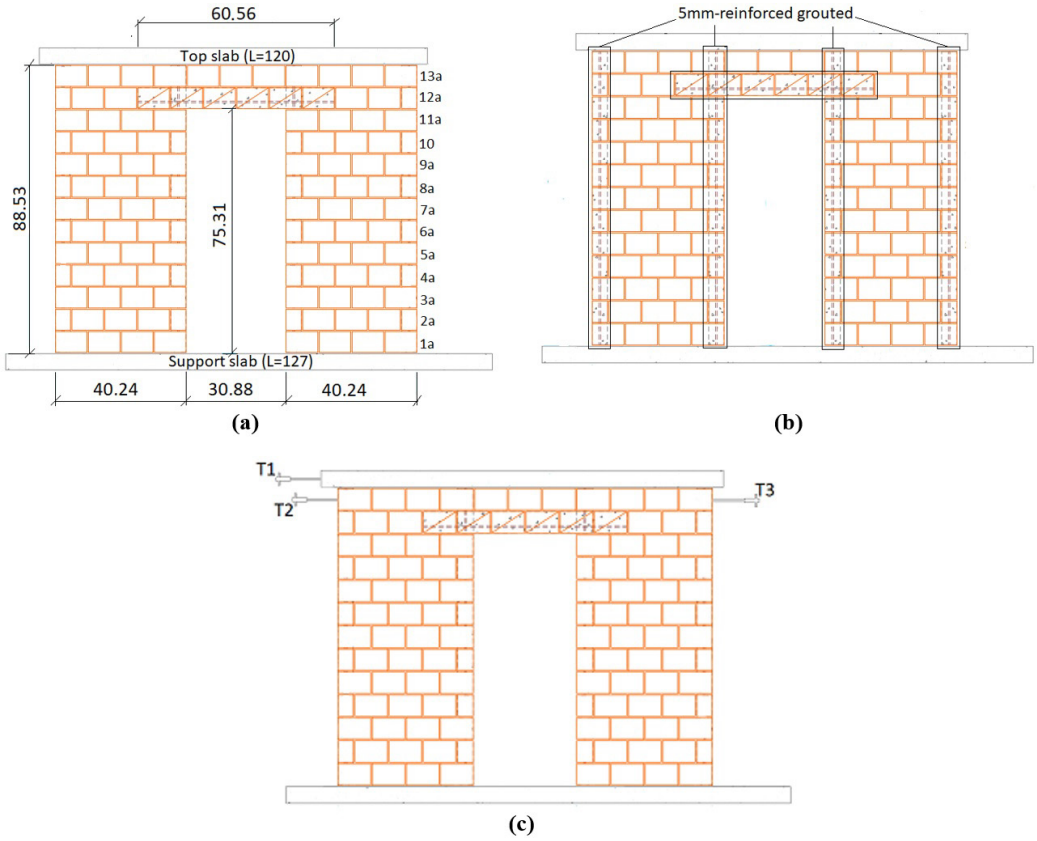


**Figure 3.** Walls with door opening. (a) PPSG1 Wall; (b) PPCG1 Wall; (c) Displacement measurement locations. Measurements in centimeters (Source: adapted from Nascimento [2]).

The experimental tests were performed using the apparatus illustrated in Figure 4 in accordance with the following procedure:

a) Previous vertical loading: three cycles of 8 kN each one was applied to the shear wall;

b) Vertical load referring to the pre-compression: vertical force equals to 30.5 kN were applied to obtain pre-compression equals to 1.64 MPa;

c) Monotonically horizontal force was applied to the shear wall reaches the total collapse.

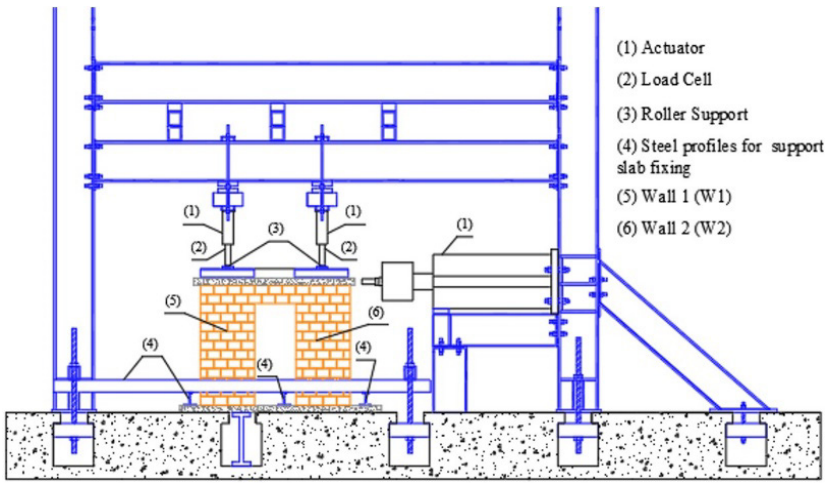


**Figure 4.** Test apparatus for shear walls.

### 3.2 Walls modeling

Computational modeling was performed by applying the equivalent frame method (EqFM), using SAP2000 software. Discretization consisted of arranging vertical bars at each block hole and horizontal bars in the mortar joints. The top slab was simulated using a horizontal bar with the properties of the reinforced concrete used in the test. The horizontal and vertical displacements were restrained at the base of the wall to simulate its support in the laboratory reaction slab. The spacing of the bars and the dimensions of the sections that each represents are shown in Figure 5. The bars in the numerical model are represented by the classical beam elements with six degrees of freedom in the ends and linear approximation for displacements function, as mentioned before. More details about the models can be found in Oliveira [22].

#### 3.2.1 Model 1 and Model 2

In Model 1, which represents the PISG1 Wall, only vertical bars with non-grouted masonry properties were used (Figure 5a). In Model 2, which represents the PICG1 Wall, bars with grouted masonry properties were also inserted in the position of the end holes, in addition to bars with the elastic properties of steel arranged beside the grouted bars (Figure 5b). Model 2 also displays a variation, divided into Model 2a, which considers reinforcement on the tensioned and compressed sides, and Model 2b, which considers reinforcement only on the tensioned side (right side).

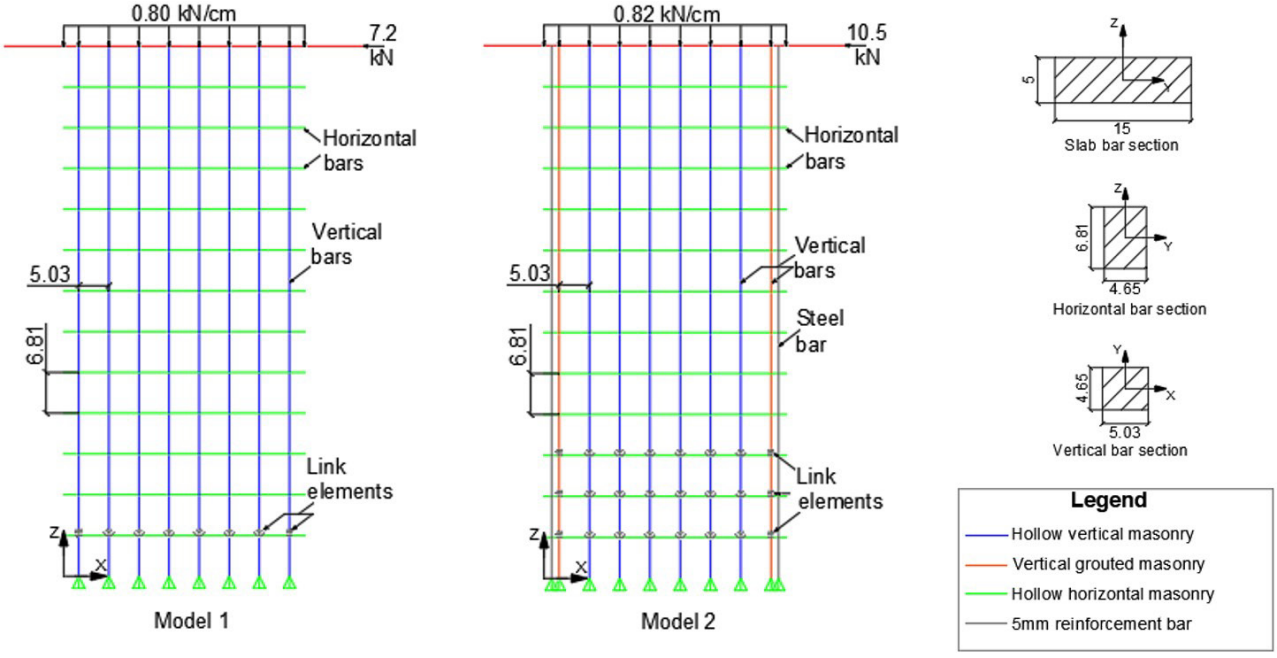


**Figure 5.** Representation of Models 1 and 2 with the cross sections and applied load. (Dimensions in centimeters).

In the SAP2000 software there are link elements available in its element library, which exhibit the length defined by the distance between the two nodes that will be connected by this element. Each type of link allows specific degrees of freedom to be associated with a linear or non-linear analysis, as well as the force-displacement law possible for each degree [16]. Thus, to simulate the effect of cracking on mortar joints, a combination of two links available in the software was selected: the GAP and the T/C Friction Isolator (T/C-FI).

The GAP element only allows compression stresses, leaving it completely free for separation between the nodes to occur in the normal direction along the contact line without mobilizing any type of bond and/or degree of freedom. The T/C Friction Isolator element allows the occurrence of both tensile and compression stresses in the normal direction along the contact line, in addition to the insertion of resistance parameters in the other two orthogonal directions, making it possible to consider the shear resistance. These two types of link elements were used in the simulations.

The link elements were positioned based on the behavior observed in the tests. In the case of the PISG1 wall, cracking was restricted to the horizontal joint at the base. Thus, in the computational model that represents this wall (Model 1), the link elements were introduced just above the first course, as illustrated in Figure 5a. With respect to the elastic properties, since the PISG1 wall was not grouted, the modulus of elasticity of non-grouted masonry in the gross area of the section (6165 MPa), obtained experimentally by Nascimento [2] was used.

The authors comment that for walls quite different from the ones evaluated in this study, the links allocation can be defined from a previous numerical simulation, observing the occurrence of tensile stresses.

In relation to the PICG1 wall, several configurations for the link elements were evaluated before obtaining the one illustrated in Figure 5b. The presence of grouting and vertical reinforcement at the ends of the section resulted in excessive stiffness when adopting the same configuration as in Model 1, making some adjustments necessary. These modifications involved using link elements in the first three courses, consistent with the cracking observed in the test. Two vertical bars were used at the ends, one simulating grouted masonry with the presence of link elements to simulate the occurrence of separation/cracking between courses, and another simulating the reinforcement, in which no link elements were included, allowing the continuity of the reinforcement and the transfer of stresses through the crack (Figure 5b). Thus, in addition to reducing the stiffness of the computational model, the intention was to simulate the cracking that occurred in the first three courses during the PICG1 wall test.

A combination of two connecting elements was used because in tests performed using only the GAP in all the bars of a course, shear stress distribution in the model was incompatible with that obtained in the test, since the GAP only works under compression and the test also involved application of horizontal forces, thereby causing shear stress. The exclusive use of the T/C FI caused the more flexible Model 1 not to resist the addition of horizontal loading and showed inconsistent displacement before reaching the collapse load obtained in the test. Thus, the T/C FI element was used only in the internal vertical bars of the two models and the GAP in the external vertical bars (Figure 6). Regarding nodes where link elements were not used, the bars are completely connected.

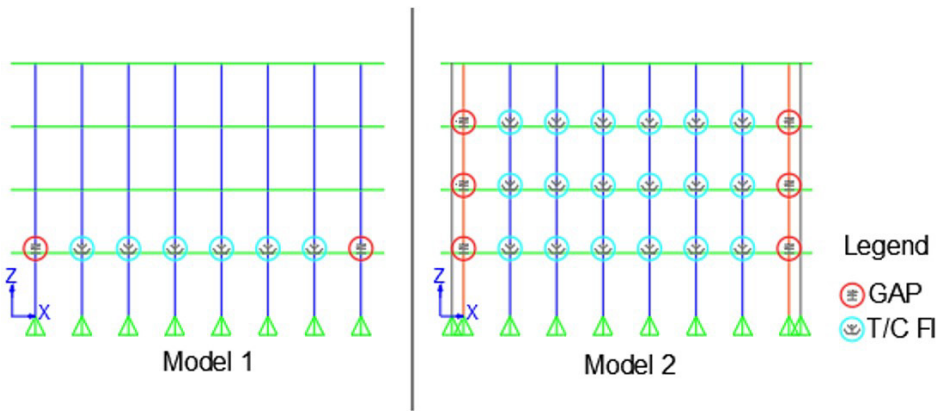


**Figure 6.** The first 4 courses of Models 1 and 2 with the position of GAP and T/C FI elements

### 3.2.2 Models 3 and 4

Models 3 and 4 refer to the modeling of walls PPSG1 and PPCG1, respectively, and were created by connecting the individual walls discretized by Models 1 or 2 using a lintel. With respect to Model 3, a combination of two Model 1 walls was used, denominated W1 and W2 for each of the wall regions (Figure 7a). According to Nascimento [2], different elastic moduli were established for the two regions from measurements taken on the wall during vertical loading, namely 8099 MPa and 4831 MPa for regions W1 and W2, respectively.

In Model 4, the combination consisted of two walls similar to Model 2, adopting the same name for the wall regions (Figure 7b). Based on the previous justification, W1 and W2 were assigned a modulus of elasticity equals to 8007 MPa and 9377 MPa, respectively, obtained from Nascimento [2]. The difference between these models and Models 1 and 2 is that only the T/C Friction Isolator link element was used, instead of combining it with the GAP element. In the tests performed, this configuration proved to be sufficient and satisfactory in tests with walls PPSG1 and PPCG1.

With respect to properties associated with GAPs and T/C FIs, as mentioned above, stiffness can be assigned at each degree of freedom direction. The nonlinear behavior and properties of the GAP were defined in relation to the vertical

direction of the wall (U1), axial to its cross section, since this is the direction of the cracks in the mortar joints. For T/C FI, in addition to the properties related to the axial direction, those pertaining to the transverse direction (U2) were also defined, in the same direction as the horizontal force applied. A summary of the properties is shown in Table 1.

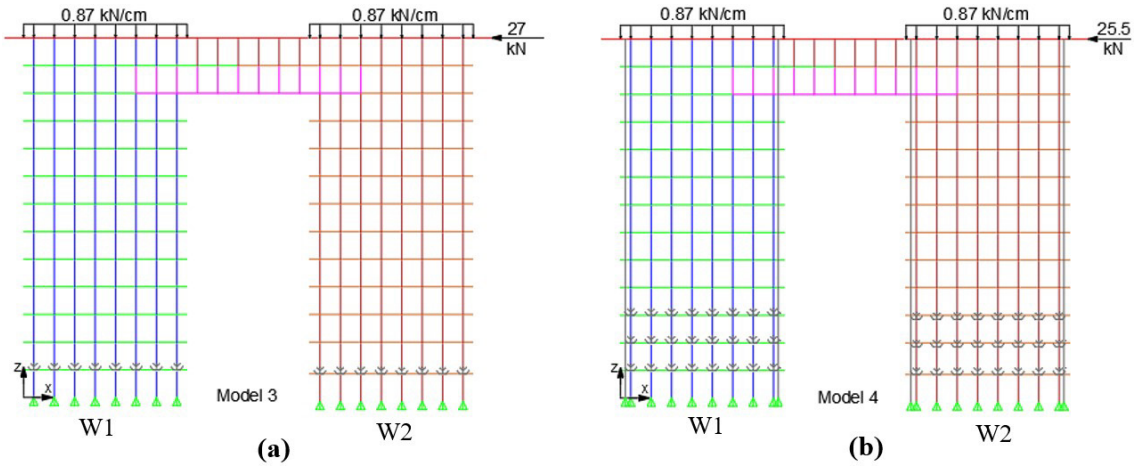


**Figure 7.** Loading illustration for Models 3 and 4

**Table 1.** GAP and T/C Friction Isolator property elements

| Property | GAP | T/C FI |
|---|---|---|
| Compressive stiffness ($k_{U1}$) (kN/cm) | 2117.42 | 2117.42 |
| Tensile stiffness ($k_{U1}$) (kN/cm) | - | 0 |
| Transverse stiffness ($k_{U2}$), when U1 refer to Tension or Compression (kN/cm) | - | 179.65 |
| Opening (cm) | 0 | 0 |
| Friction coefficient | - | 1 |

The compressive stiffness ($k_{U1}$) was determined from the classical strength of materials theory (Equation 1).

$$k_{U1} = \frac{EA}{L} \tag{1}$$

In which: $E$ is the longitudinal elasticity modulus of non-grouted masonry; $A$ represents the cross-sectional area of a masonry bar; $L$ is the length of a masonry bar.

The transversal stiffness value ($k_{U2}$) was calculated by Equation 2, which refers to the inverse of the displacement due to shear force, according to the classical concepts of structural theory.

$$k_{U2,U3} = \frac{G_a \times A}{c \times H} \tag{2}$$

In Equation 2, $G_a$ is the transversal elasticity modulus obtained from Equation 3:

$$G_a = \frac{E_a}{2 \times (1+\nu)} \tag{3}$$

In which: $E_a$ is the longitudinal elasticity modulus of non-grouted masonry; $\nu$ is the coefficient of poisson; $A$ represents the cross-sectional area of a masonry bar; $c$ is a corrective factor of the shear stress distribution (equals to 1.2 for rectangular sections); and $H$ is the height of the wall.

About the initial null opening value, tests that varied this parameter found no influence on the results obtained. This was expected, since this parameter is associated with the mobilization of degrees of freedom corresponding to compressive stresses, and the nonlinearity evaluated is related to the mobilization of tensile stresses. A length of 1.0 cm was adopted for the link elements because lower values resulted in numerical inconsistency. The friction coefficient was obtained from preliminary analyzes performed by the authors, varying this parameter between 0.5 and 1.0. The tests results showed that this coefficient did not have much influence. Therefore, based on recommendations from

Canadian Standards Association (S304-14) [23] and the studies of Parsekian et al. [3] and Pasquantonio et al. [24], the authors decided to adopt 1.0 as the value of the friction coefficient. In their work, Pasquantonio et al. [24] presents a table with five other references about the coefficient of friction at the interface between masonry and mortar. The average value of the coefficient of friction (μ) founded by those researchers was equal to 1.07, while the value of 0.61 was obtained by Pasquantonio et al. [24] in the experiments carried out in their research.

### 3.3 Loading Cases

Given that the purpose of computational modeling was to evaluate the reduction of wall stiffness caused by cracking, loading was applied incrementally. Thus, a combination of geometric nonlinear loading was used, consisting of vertical loading and horizontal forces (Figure 5). All the models were submitted to pre-compression equals to 1.64 MPa corresponding to vertical load equals to 0.80 kN/cm and 0.82 kN/cm for Models 1 and 2, respectively. The horizontal forces were incrementally applied to the computational model up to collapse load achieved in the test, with intensities of 7.2 kN and 10.5 kN, corresponding to Models 1 and 2, respectively. Models 3 and 4 were submitted to a vertical load of 0.87 kN/cm on each of the regions. The maximum horizontal load applied in Models 3 and 4 was 27 kN and 25.5 kN, respectively (Figure 7). Thus, the following procedure was adopted for the loads considered in the computational models:

- Exclusive application of vertical loading to obtain the initial state of compressive stresses in the walls.
- Based on the initial stress state in the wall, horizontal force was introduced in 1.0 kN increments, up to the maximum value obtained in each of the tests. The aim was to induce the formation and propagation of cracking in the wall and incrementally assess the progressive lack of stiffness.

It is important to emphasize that no non-linear behavior was considered for the masonry materials; only the effects arising from cracking in the horizontal mortar joints were evaluated.

## 4 RESULTS AND DISCUSSIONS

### 4.1 Analysis of horizontal displacements

According to Nascimento's study [2], the horizontal displacements measured by transducers T1 and T2 were used for comparison purposes with the results of computational models, as illustrated in Figure 2c, associated with the top slab and the top masonry course, respectively. In the following graphs (Figure 8 and Figure 9), the solid lines represent the experimental results (Exp.), and the dashed lines the computational modeling results.

#### 4.1.1 Results of unreinforced walls

Figure 8 illustrates the horizontal displacements associated with walls PISG1 and PPSG1. According to Nascimento [2], in the case of PISG1, linear behavior was characterized as the horizontal force ranged between 1 kN and 3.5 kN, after which nonlinear behavior was identified and intensified after the first visible crack at 5.7 kN. According to the author, total wall failure occurred with a horizontal force intensity of 6.7 kN. Nascimento [2] also reports that the horizontal section of the curve corresponds to a rigid body movement which, in turn, may be associated with hinge formation at the base of the wall, where residual resistance could be linked to the formation of a diagonal strut. Under these stress distribution conditions; the wall was already about to fail.

As can be seen in Figure 8a, the numerical model displayed a tendency to behave similarly to its experimental counterpart, despite being more flexible. A section with linear behavior is observed until the intensity of the horizontal force reaches 3.5 kN, with initial nonlinear behavior between 3.5 kN and 4.8 kN, whose effect intensified from 5.0 kN onwards, just before the experimental result. The maximum displacement achieved with the computational model was 8.84 mm, in transducer 1, 1.7 times higher than that recorded in the test, equals to 5.2 mm. This greater flexibility in the computational model can be attributed to its simpler simulation using discrete elements (bars), which therefore may not represent smooth crack propagation. Another factor that could have influenced stiffness in the computational model is the greater complexity of simulating a non-reinforced element, which can make it difficult to achieve equilibrium during nonlinear processing. The results obtained with the computational model corroborate Nascimento's description [2], in which he considered a main crack in the base as the most important part of nonlinear wall behavior.

One aspect that was not well represented in the computational result was the rigid body movement described by the author of the tests. This effect is difficult to simulate, especially when plasticity and/or rupture criteria are not used for masonry, leaving these aspects to be explored in future research. Nevertheless, the proposed model did yield the final objective, which was the simulation of stiffness degradation from the cracking process at the base of the wall.

Furthermore, for the purpose of evaluating stiffness lack in building walls, the model exhibits result that favor safety, since a greater lack is estimated than that obtained experimentally.

The results obtained for wall PPSG1 (Figure 8b) showed the same tendency as those of PISG1, where the computational model was more flexible than its experimental counterpart, whose collapse was occurred with a horizontal force of 24 kN. In contrast to what occurred with PISG1, the maximum displacements associated with the computational model were close to those obtained experimentally. This result may be attributed to less cracking in the wall region to the left of the opening, as described by Nascimento [2], thereby reducing the effects of wall stiffness lack and making the assembly less unstable and the computational simulation less complex. According to the author, linear behavior is acceptable up to a horizontal force of 15 kN, after which nonlinear behavior is observed, intensifying at 18 kN after the first visible crack. Model 3 shows linear behavior up to approximately 11 kN of horizontal force, where nonlinearity is characterized, intensifying from 15 kN onwards, results similar to those obtained experimentally. As previously mentioned, including plasticity and/or rupture criteria may further improve these results, which could be investigated in future research.

With respect to the models with no reinforcement or vertical grouting, it should be noted that building codes stipulate the use of reinforcement whenever tensile stresses occur in the structural walls. The results presented here do not apply to unreinforced shear wall situations with tension loads. The aim is to validate the computational modeling proposed based on the behavior of a difficult computational simulation due to the absence of vertical reinforcement.

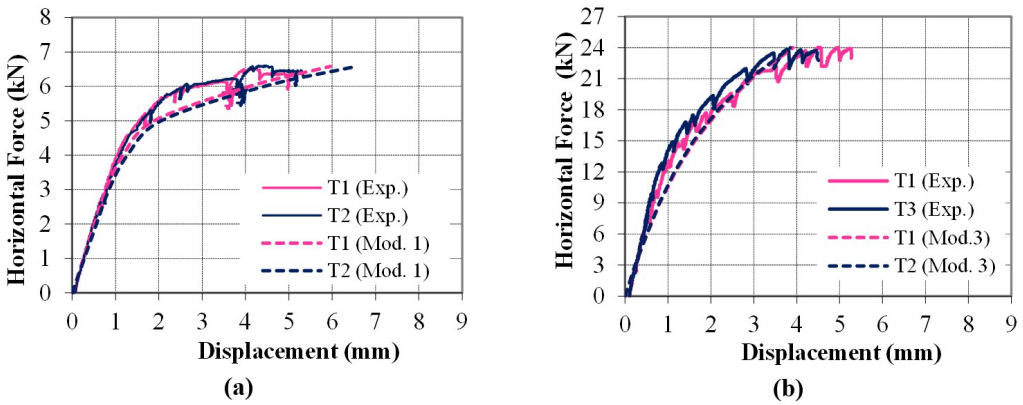


**Figure 8.** Horizontal force × horizontal displacement graph: (a) PISG1 Wall and Model 1; (b) PPSG1 Wall and Model 3.

### 4.1.2 Results of reinforced walls

Figure 9 illustrates the results of walls PICG1 and PPCG1. With respect to the experimental results for PICG1, Nascimento [2] found that the linear section was formed between horizontal forces of 1.0 kN and 4.5 kN, followed by the onset of nonlinear behavior, with the first visible crack observed at 7.0 kN. According to the author, the wall failed at a horizontal force intensity of 10.5 kN and, unlike PISG1, without the occurrence of rigid body movement and the appearance of a horizontal section in the curve. The absence of the horizontal section, lower stiffness lack, and greater horizontal failure load of PICG1 in relation to its PISG1 counterpart may be attributed to the effect of grouting and vertical reinforcement at the ends. In contrast to PISG1, cracking in PICG1 occurred in three courses at the base, underscoring the effect of vertical reinforcement on the transfer of tensile stresses through these cracks.

Two Model 2 configurations were assessed, considering or not reinforcement at the compressed end of the wall. This variation in the computational model was based on the study conducted by Camacho et al. [25], Oliveira [22], who found that different reinforcement ratios did not influence the compressive strength of concrete block prisms. The results obtained showed no significant differences, except for the section after a horizontal force of 9.0 kN was applied, where the model without compressed reinforcement showed more intense nonlinearity. Thus, only the results of the model with compression reinforcement were displayed.

Comparison of the results obtained for Model 2 and wall PICG1 demonstrated statistically similar absolute values. Assessment of the initial linear section of the computational model revealed that it was limited by the intensity of the horizontal force of approximately 4.0 kN, 11.31% below the experimental value. Intensified nonlinear behavior was identified starting at a force of 6.0 kN, a value 14.3% lower than that associated with the appearance of the first visible

crack during the test. PICG1 failed at a top displacement of 6.2 mm, while Model 2 resulted in a top displacement of 5.71 mm, corresponding to a difference of -7.9%.

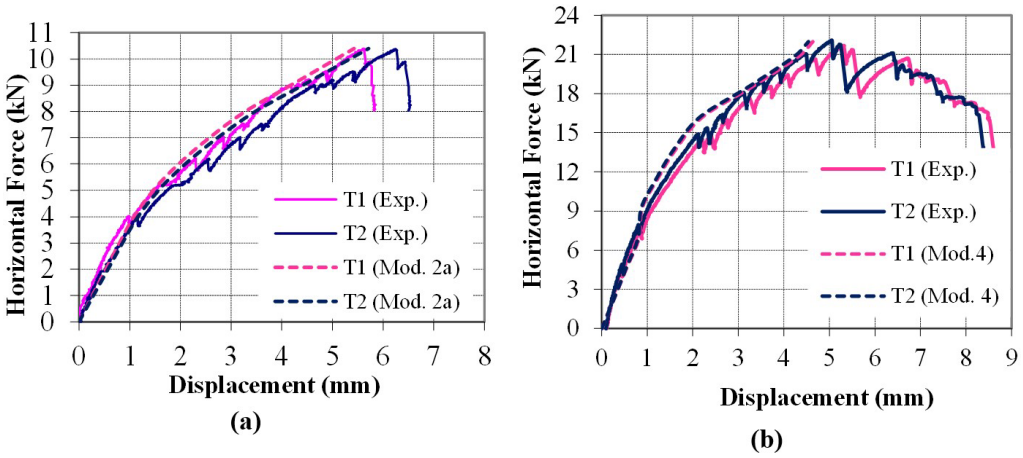


**Figure 9.** Horizontal force × horizontal displacement graph: (a) PICG1 Wall and Model 2; and (b) PPCG1 Wall and Model 4.

About the PPCG1 wall, the similarity between the results of the computational (Model 4) and experimental models is also significant. As reported by Nascimento [2], greater stiffness lack occurred starting at 18 kN and the test reached a maximum horizontal force intensity of 22 kN. Model 4 shows that intensification began at approximately 16 kN (11.1% lower). The post-peak sections observed in the experimental results could not be simulated in the computational model, and since the main objective was to evaluate the lack of stiffness from cracking, failure and plasticity criteria were not considered for masonry in this study.

### 4.2 Analysis of normal stress distribution in computational modeling

#### 4.2.1 Models 1 and 3

Analysis of normal stress distribution is associated with the corresponding models submitted to the maximum intensity of the horizontal force measured in the tests, namely 7.2 kN in Model 1 and 27 kN in Model 3. Figure 10 illustrates the normal force distribution in Model 1, on computational modeling (Figure 10a) and experimental tests (Figure 10b). As expected, compressive forces were concentrated on the left edge of the wall, increasing from the top to the base, suggesting the formation of a diagonal strut. Figure 10c illustrates the stress distribution at the base of the wall, showing a section to the left with a region subjected to compressive stresses in the base course, with a maximum intensity of -1.33 kN/cm$^2$, a long central stress-free section, associated with the horizontal crack in the mortar joint, and, finally, very low tensile stresses at the other end of the wall. A horizontal cross section in the second course of the wall showed no tensile stresses, indicating adequate simulation of cracking in the horizontal joint.

In relation to Model 3, Figure 10a-10b demonstrate the normal stress distribution, with a formation of a possible diagonal strut in the region of the wall to the left of the opening, starting from the upper right corner at the connection point with the lintel, towards the lower left corner at the base of the wall. In the region on the right, there is a small concentration of compressive stresses in the lower left corner, and a section at the top of the wall with high intensities caused by horizontal forces. Stress distribution in horizontal cross sections at the base of this wall, as seen in Figure 11c, was consistent with the cracking observed during the test. No stress occurred over most of the cross section of the wall region to the right of the opening, which was subjected to compressive stress equivalent to the length of only one block. In the wall region to the left of the opening, the stress-free region was limited to nearly half the width of the region, where the region submitted to compressive stresses exhibited maximum intensities 2.50 times greater than those of the other wall region.

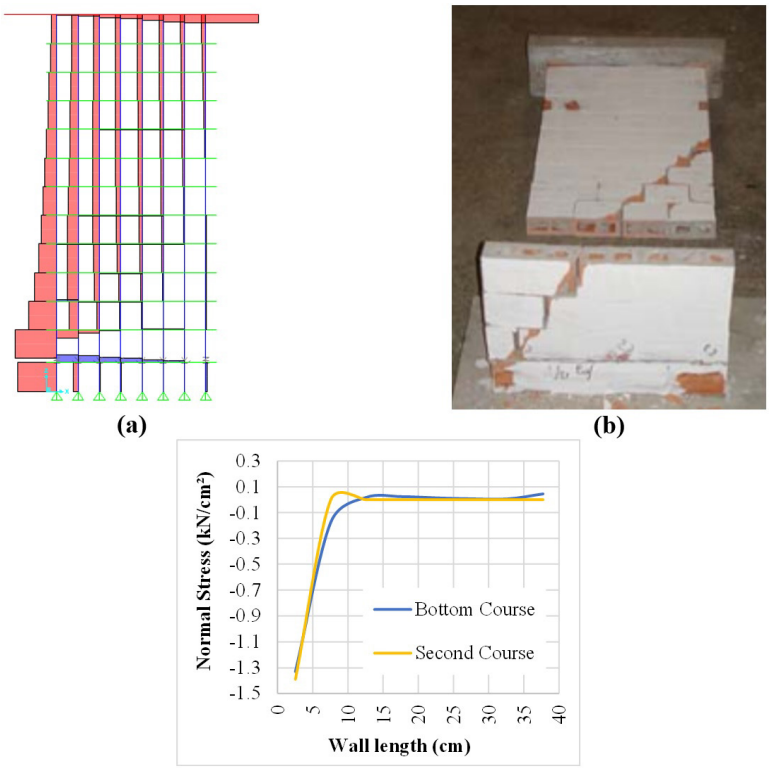


**Figure 10.** Normal stress distribution in Model 1: (a) Computational Modeling; (b) Experimental Test; (c) Normal stress distribution in the base cross sections.

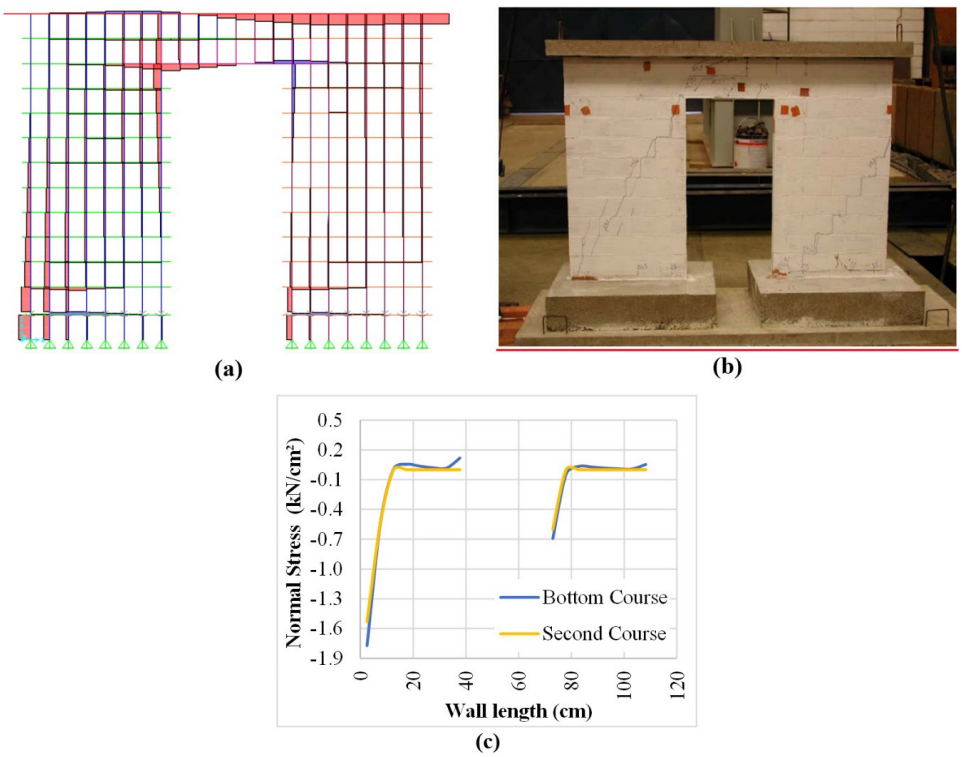


**Figure 11.** Normal stress distribution in Model 3: (a) Computacional Modeling; (b) Experimental Test; (c) Normal stress distribution in the base cross sections.

### 4.2.2 Models 2 and 4

The results exhibited below refer to the horizontal force caused by the failure of the experimental models, namely 10.5 kN in PICG1 and 25.5 kN in PPCG1. A comparison between Figure 12a-12b and the corresponding for PISG1 (Figure 9a-9b) reveals similar behavior, except for the occurrence of tensile stresses over the entire right edge of the wall, resulting from the vertical reinforcement. The beneficial effect of reinforcement in controlling cracking and thereby increasing wall stiffness is evident in the tensile stress peaks of Figure 12c, reaching yield stress in the cross-section of the second course, with continuous reduction in the tensile stress in the courses immediately above. The peaks are so high that the compressive stresses associated with the masonry become imperceptible, even in the cross-section region with vertical grouting. These stresses are only seen in Figure 12d, where stress in reinforcement was omitted. This figure also shows the occurrence of a stress-free region in cross-section, which declines with the addition of courses, associated with the occurrence of probable cracking. It is noteworthy that cracking was detected up to the third course in the wall test. The occurrence of short stress-free region in cross-sections beyond the third course is fully acceptable, since the reinforcement controls cracking, making it imperceptible. Regarding the region of cross-sections submitted to compressive stresses, in the base cross-section their extension is smaller, and the maximum intensity is higher. This tendency may be due to the greater bending moment intensity at the base, resulting in greater compressive and tensile stresses, thereby increasing maximum compressive stress and the stress-free region in cross-section, associated with crack extension in the mortar joint.

The results of Model 4 demonstrate the same trend of diagonal strut mobilization in both regions of the wall, as that observed in Model 2. The vertical reinforcement mobilization illustrated in Figure 13 shows that the reinforcement subjected to the greatest tension was in the wall region to the right of the opening, corroborating the occurrence of more intense cracking in this region. Nevertheless, yield stress was not characterized. In relation to compression reinforcement, a relevant stress intensity of 40 kN/cm$^2$ was detected in Model 2. It is important to note that the tests conducted by Camacho et al. [25] investigated prisms submitted to simple compression, which differs significantly from the axial compression with flexure applied to the walls studied here. Thus, it is necessary to reassess the effect of compressed reinforcement under stress distribution like that exhibited by the shear walls studied. It should also be noted that the modeling without compression reinforcement was evaluated and no substantial changes in stiffness were detected.

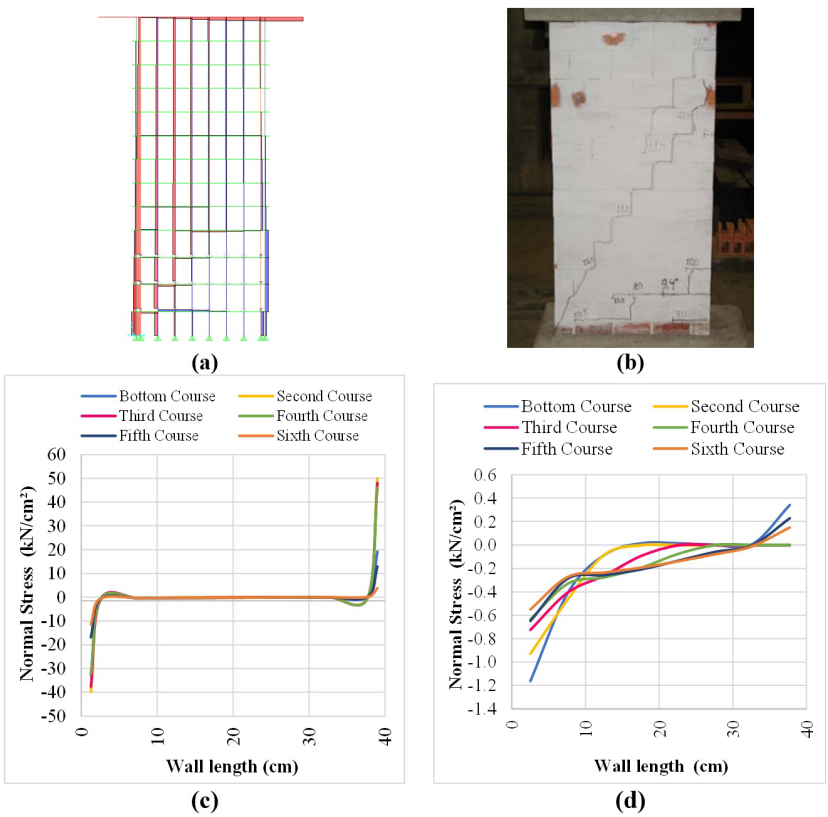


**Figure 12.** Normal stress distribution in Model 2: (a) Modeling; (b) Experimental test. Normal stress distribution in the base cross-sections: (c) with stress in reinforcement; (d) without stress in reinforcement

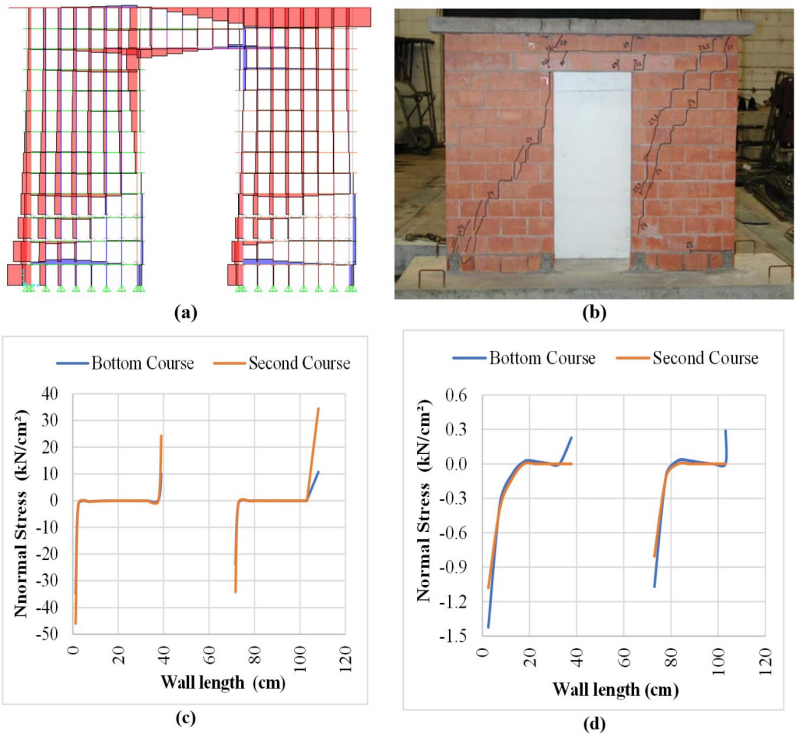


**Figure 13.** Normal stress distribution in Model 4: (a) Modeling; (b) Experimental test. Normal stress distribution in the base cross-sections: (c) with stress in reinforcement; (d) without stress in reinforcement.

## 5 CONCLUSIONS

The analyses proposed in this study consisted of using an improved equivalent frame method (EqFM) to computationally simulate the behavior of masonry shear walls subjected to horizontal and vertical loads in their own plane. The main objective was to determine the model's capacity to represent the walls stiffness degradation caused by cracking in the horizontal mortar joints. Based on the results obtained, the following conclusions could be drawn:

- The use of simple link elements that allow complete separation between the courses of the shear wall when tensile stresses occur was sufficient to simulate the initialization and propagation of cracks;
- In the shear wall without vertical reinforcement, the use of link elements associated with the first horizontal mortar joint is sufficient to represent the behavior observed, since the main cracking occurs in this joint before the wall fails;
- In the shear wall with grouting and vertical reinforcement at the ends, it is necessary to use link elements in the first three courses. Including compressive reinforcement in the modeling did not lead to significant changes in shear wall stiffness. However, its participation in stress distribution and resistance of the cross section submitted to axial compression and flexure load requires further investigation;
- The computational models developed proved to be efficient in simulating the stiffness degradation caused by cracking in the horizontal mortar joints. The numerical curves yield strong similarity with those obtained in the tests, and the computational models were always slightly more flexible and thus favor safety;
- In addition to the change in behavior between reinforced and non-reinforced shear walls, analysis of normal stress distribution in different cross-sections of the walls also indicated the efficiency of reinforcement in transferring tensile stresses between the cracks.

## REFERENCES

[1] J. A. Nascimento No., K.A.S. Medeiros, and F. Quim, “Nova modelagem para análise da interação entre painéis de alvenaria e estrutura de suporte,” *Rev. Prisma.*, vol. 3, no. 52, pp. 39–48, Maio 2014.

[2] J. A. Nascimento No., “Estudo de painéis com abertura constituídos por alvenaria estrutural de blocos,” Doctoral dissertation, Esc. Eng. São Carlos, Univ. São Paulo, São Carlos, SP, Brazil, 2003.

[3] G. A. Parsekian, A. A. Hamid, and R. G. Drysdale, *Comportamento e Dimensionamento de Alvenaria Estrutural*, 2nd ed. São Carlos, SP, Brazil: EdUFSCar, 2013.

[4] M. S. Paes, "Interação entre edifício de alvenaria estrutural e pavimento em concreto armado considerando-se o efeito arco com a atuação de cargas verticais e ações horizontais," Master thesis, Esc. Eng. São Carlos, Univ. São Paulo, São Carlos, SP, Brazil, 2008.

[5] R. C. Mata, "Análise experimental e numérica do comportamento de juntas em painéis de contraventamento de alvenaria estrutural," Doctoral dissertation, Esc. Eng. São Carlos, Univ. São Paulo, São Carlos, SP, Brazil, 2011.

[6] J. A. Nascimento No., "Investigação das solicitações de cisalhamento em edifícios de alvenaria estrutural submetidos a ações horizontais," Master thesis, Esc. Eng. São Carlos, Univ. São Paulo, São Carlos, SP, Brazil, 1999.

[7] D. I. S. Gomes, "Análise não-linear física simplificada de estruturas de contraventamento de edifícios de alvenaria estrutural," Master thesis, Esc. Eng. São Carlos, Univ. São Paulo, São Carlos, SP, Brazil, 2010.

[8] S. C. Peleteiro, "Contribuições à modelagem numérica de alvenaria estrutural," Doctoral dissertation, Esc. Eng. São Carlos, Univ. São Paulo, São Carlos, SP, Brazil, 2002.

[9] U. Andreaus, "Failure criteria for masonry panels under in-plane loading," *J. Struct. Eng.*, vol. 122, no. 1, pp. 37–46, Jan. 1996, http://dx.doi.org/10.1061/(ASCE)0733-9445(1996)122:1(37).

[10] G. P. A. G. van Zijl, "Modeling masonry shear-compression: role of dilatancy highlighted," *J. Eng. Mech.*, vol. 130, no. 11, pp. 1289–1296, Nov. 2004.

[11] A. Gabor, E. Ferrier, E. Jacquelin, and P. Hamelin, "Analysis and modelling of the in-plane shear behaviour of hollow brick masonry panels," *Constr. Build. Mater.*, vol. 20, pp. 308–321, Mar. 2005, http://dx.doi.org/10.1016/j.conbuildmat.2005.01.032.

[12] A. Zucchini and P. B. Lourenço, "A micro-mechanical homogenisation model for masonry: application to shear walls," *Int. J. Solids Struct.*, vol. 46, pp. 871–886, Oct. 2008, http://dx.doi.org/10.1016/j.ijsolstr.2008.09.034.

[13] K. A. S. Medeiros, "Modelagem computacional para avaliação da interação entre painéis de alvenaria e estrutura de suporte em concreto armado," Master thesis, Prog. Pós-grad. Eng. Civil, Univ. Fed. Rio Grande do Norte, Natal, RN, Brazil, 2015.

[14] A. C. S. Lopes, "Aperfeiçoamento de modelagem computacional para análise da interação entre painéis de alvenaria e estrutura de suporte em concreto armado," Undergraduate thesis, Dept. Eng. Civil, Univ. Fed. Rio Grande do Norte, Natal, RN, Brazil, 2016.

[15] Y. Belmouden and P. Lestuzzi, "An equivalent frame model for seismic analysis of masonry and reinforced concrete buildings," *Constr. Build. Mater.*, vol. 23, no. 1, pp. 40–53, Jan. 2009, http://dx.doi.org/10.1016/j.conbuildmat.2007.10.023.

[16] K. C. Voon and J. M. Ingham, "Experimental in-plane strength investigation of reinforced concrete masonry walls with openings," *J. Struct. Eng.*, vol. 134, no. 5, pp. 758–768, May 2008.

[17] H. Pirsaheb, P. Wang, M. J. Moradi, and G. Milani, "A Multi-Pier-Macro MPM method for the progressive failure analysis of perforated masonry walls in-plane loaded," *Eng. Fail. Anal.*, vol. 127, p. 105528, Sep. 2021.

[18] H. Pirsaheb, P. Wang, M. J. Moradi, and G. Milani, "A Multi-Pier MP procedure for the non-linear analysis of in-plane loaded masonry walls," *Eng. Struct.*, vol. 212, p. 110534, Jun. 2020.

[19] M. P. Barbosa, "Estudo da interação entre grupos de paredes na distribuição das cargas verticais em edifícios de alvenaria estrutural," Undergraduate thesis, Dept. Eng. Civil, Univ. Fed. Rio Grande do Norte, Natal, RN, Brazil, 2017.

[20] I. C. Guerrante, "Análise numérica de vigas de concreto armado reforçadas por encamisamento parcial," Master thesis, Prog. Eng. Civil, COPPE, Univ. Fed. Rio de Janeiro, Rio de Janeiro, RJ, Brazil, 2013.

[21] M. L. F. Simões, "Reforço à flexão de vigas de concreto armado por encamisamento parcial," Master thesis, Prog. Eng. Civil, COPPE, Univ. Fed. Rio de Janeiro, Rio de Janeiro, RJ, Brazil, 2007.

[22] N. N. S. Oliveira, "Análise de paredes de contraventamento de alvenaria estrutural de blocos de concreto considerando os efeitos da fissuração," Master thesis, Prog. Pós-grad. Eng. Civil, Univ. Fed. Rio Grande do Norte, Natal, RN, Brazil, 2021.

[23] Canadian Standards Association, *Design of Masonry Structures, CSA S304-14*, 2014.

[24] R. D. Pasquantonio, G. A. Parsekian, F. S. Fonseca, and N. G. Shrive, "Experimental and numerical characterization of the interface between concrete masonry block and mortar," *Rev. IBRACON Estrut. Mater.*, vol. 13, no. 3, pp. 578–592, Jun. 2020, http://dx.doi.org/10.1590/S1983-41952020000300008.

[25] J. S. Camacho, B. G. Logullo, G. A. Parsekian, and P. R. N. Soudais, "Influência do graute e da taxa de armadura no comportamento à compressão da alvenaria de blocos de concreto," *Rev. IBRACON Estrut. Mater.*, vol. 8, no. 3, pp. 341–364, Jun. 2015, http://dx.doi.org/10.1590/S1983-41952015000300006.

**Author contributions:** NNSO: conceptualization, formal analysis, methodology, writing; JANN and GAP: conceptualization, supervision, revising.

**Editors:** Tulio Nogueira Bittencourt, Antônio Carlos dos Santos.